Supplementary Information

Antibody-functionalized MXene-based electrochemical biosensor for point-of-care detection of vitamin D deficiency

Sharat Chandra Barman[1], Yuming Jin[1], Jehad K. El-Demelawi[2], Simil Thomas[1], Nimer Wehbe[3] , Yongjiu Lei[1], Mrinal Kanti Hota[1,4], Xiangming Xu[1], Erol A. Hasan[1], Omar F. Mohammed[1,2], Osman M. Bakr[1,2], Dana Alsulaiman [ID] 1*, and Husam N. Alshareef [ID]1'2*

[1]Materials Science and Engineering, Physical Science and Engineering (PSE) Division, King Abdullah University of Science and Technology (KAUST), Thuwal, 23955, Saudi Arabia

[2]*Center for Renewable Energy and Storage Technologies (CREST), King Abdullah University of Science and Technology (KAUST), Thuwal 23955-6900, Saudi Arabia*

[3]Core Labs, King Abdullah University of Science and Technology (KAUST), Thuwal, 23955, Saudi Arabia

[4]Materials Research Laboratory, University of Illinois at Urbana Champaign, 104 S. Goodwin Ave., 61801, Urbana, Illinois, United States

*Email: dana.alsulaiman@kaust.edu.sa, husam.alshareef@kaust.edu.sa

Contents

Materials and Methods

Human Serum Samples and Bioethics Approval

Serum from human male AB plasma was purchased commercially from Sigma-Aldrich (H4522-100mL). The protocol detailing the serum usage was approved by the KAUST Institutional Bioethics and Biosafety Committee under protocol 22IBEC028.

Synthesis and Preparation of $Ti_3C_2T_x$ (MXene) and MXene-PEI

MXene was synthesized based on our previous protocol.[1] Briefly, 1 g Ti_3AlC powders were added into 12 mL etching solution containing HCL: HF: (HF aqueous solution (49%, Sigma-Aldrich): DI water at a volume ratio of (3:6:3) at 55 °C for 16 h with magnetic stirring in oil bath. The as-prepared suspension was washed multiple times with deionized water by several rounds of centrifugation and decantation until a pH reached 6−7. Following this, the solution underwent multiple cycles of centrifugation/decantation until reaching a pH range of 6-7. Next, 1.2 grams of lithium chloride (LiCl, obtained from Sigma-Aldrich) were combined with the sediment in 40 milliliters of deionized water (DI). The mixture was gently agitated for 30 minutes to facilitate the intercalation of LiCl. Subsequently, the MXene suspension containing LiCl was subjected to additional rounds of centrifugation and decantation to achieve a pH range of 6-7. The final sediments were redispersed in deionized water and centrifuged at 6000 rpm for 5 min for collection. The supernatant solutions were collected and used for the thin film preparation by vacuum filtration. The films were dried overnight under a high vacuum and used for characterization.

After the successful synthesis of MXene (approximately 2mg/ml), it was redispersed in Poly(ethyleneimine) solution (Sigma Aldrich, 50% in water) at the ratio of (3 mL: 100 µL), respectively and stirred for 2h in room temperature to get MXene-PEI.

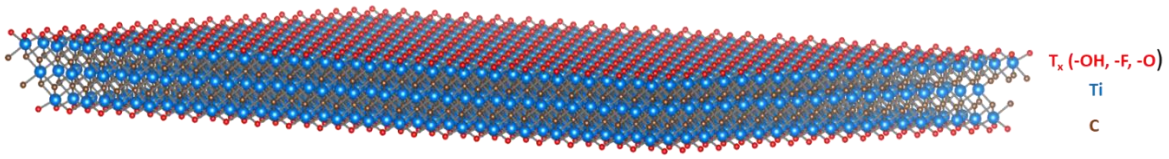

Figure S1. Schematic illustration of a $Ti_3C_2T_x$ (MXene) single sheet with T_x indicating the surface-terminated functional groups (-O, -OH, -F).

Materials Characterization

X-ray diffraction (XRD)

XRD analysis of the MXene nanosheet was performed with a powder X-ray diffractometer (Bruker D8 Advance) using Cu Kα radiation at a wavelength of 1.5418 Å. The scanning rate was 0.5 s/step at a step size of 0.02° in the 2θ range of 5°- 45°.

Raman Spectroscopy

Raman spectra were obtained using a micro-Raman spectrometer (Witec Apyron) outfitted with a 532 nm wavelength cobalt blue laser and an Olympus 50× objective lens.

Atomic force microscopy (AFM)

Atomic force microscopy (AFM, Bruker, Dimension Icon SPM) was employed to capture surface morphologies and thickness profiles of the manufactured MXene flakes. These MXene nanosheets were dispersed onto glass substrates via random spraying, subsequently dried under vacuum conditions, and rinsed with DI water to prepare samples for AFM analysis.

Transmission electron microscopy (TEM)

High-resolution TEM images were acquired using the FEI Titan 80-300 ST (U.S.).

X-ray photoelectron spectroscopy (XPS)

XPS data were obtained using a Kratos Axis Supra instrument equipped with a monochromatic Al Kα X-ray source (hv = 1486.6 eV) operating at a power of 75 W and under UHV conditions in the range of $\sim 10^{-9}$ mbar. All spectra were recorded in hybrid mode, using electrostatic and magnetic lenses and an aperture slot of 300 μm × 700 μm. The wide and high-resolution spectra were acquired at fixed analyzer pass energies of 80 eV and 20 eV, respectively. The samples were mounted in a floating mode to avoid differential charging.

Universal laser system VLS3.75, 75 watts CO_2 (used scanning parameters- power 2.7% speed 2.5%, PPI 1000, Z-axis 2.00 mm).

Dynamic Light scattering (DLS)

DLS Zeta sizer (Malvern Nano-ZS 3600) measurement parameters-10 round measurement, in the presence of water solvent, at 22 ° C and using transparent disposable Dip cell cuvette. MXene solution was diluted by 12 times in DI water.

Dynamic light scattering characterization

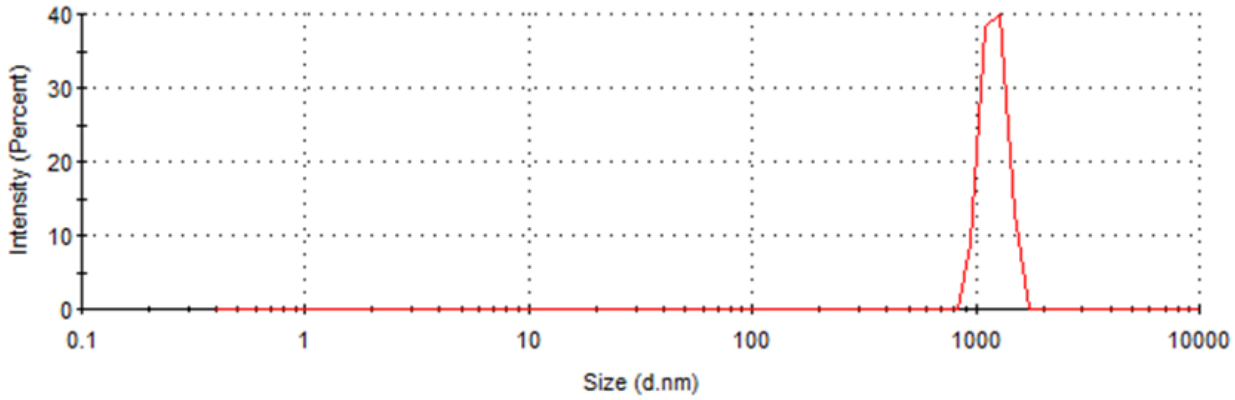

Figure S2. MXene Particle size measurement using Malvern Dynamic Light scattering (DLS) Zeta sizer.

Sensor Design and Fabrication

The sensor was developed following our previous protocol[2], designed as a smartphone-compatible readout-based sensor. The exact dimensions of the working electrode (WE), counter electrode (CE), and reference electrode (RE) are illustrated in **Figure S3(a)** designed using **AutoCAD** 2023 (Student version). The Polyimide film, with a 0.125 mm thickness, was patterned by CO_2 laser. After that, the Ag/AgCl ink (Cat: 011464, BAS Inc. Japan) was drop-cast on the reference electrode and cured at 80 °C for 1 hour. Laser-induced graphene was directly utilized as the counter electrode. After that, the unnecessary electrode area is passivated by a glue gun.

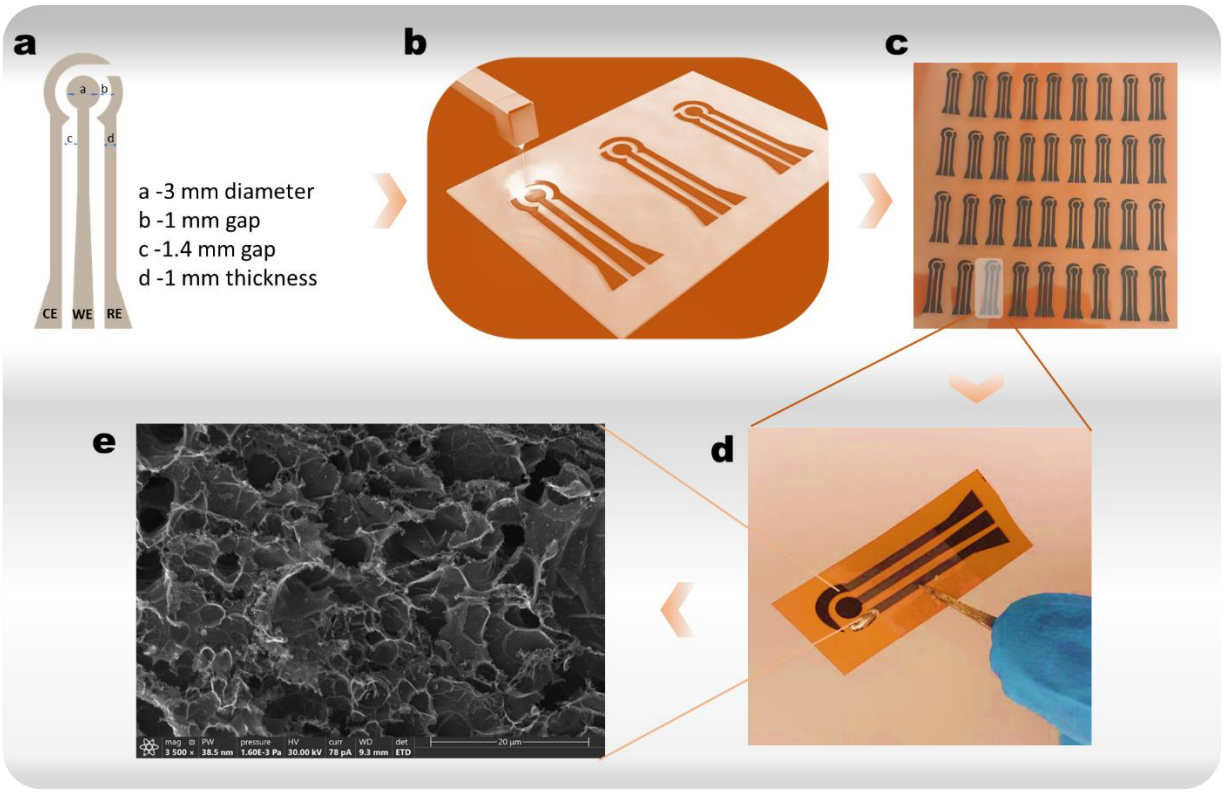

Figure S3. a) CAD design, b) Schematic for the electrode fabrication by CO_2 laser writing, c) photograph of the fabricated electrodes, d) Ag/AgCl pasting on the reference electrode and passivating the unnecessary part, and e) SEM image of the as-prepared laser-induced graphene electrode.

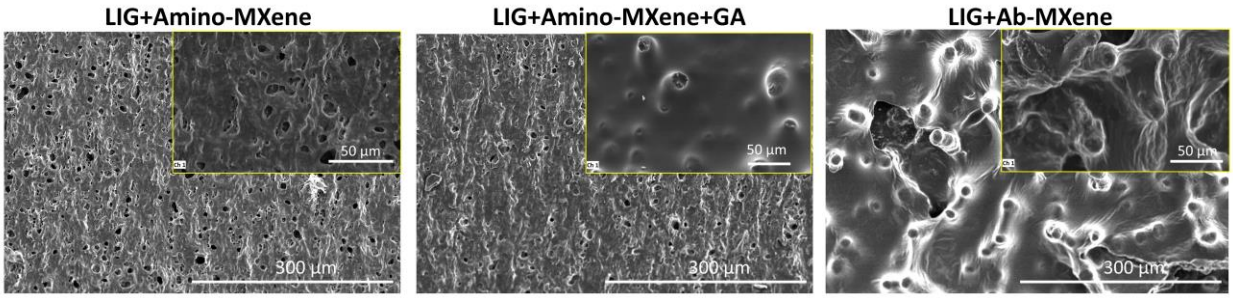

Figure S4. SEM micrographs of LIG+Amino-MXene, LIG+Amino-MXene+GA, and LIG+Ab-MXene with a zoom-out view to better illustrate the sample morphology and structure. A Zoom-in view is shown in the inset outlined by the yellow box.

Vit-D Sensor Preparation

The as-prepared Mxene-PEI solution (3 µl) was drop-cast onto the working area and dried under N_2 gas overnight. The sensor was treated with glutaraldehyde 5% (GA) solution for 4h, followed by washing with 1X PBS to remove unbound GA. After that, the Vit-D antibody solution (10 µg/ml) was drop-cast onto the working electrode and subsequently washed with PBS solution. Bovine serum albumin solution (5%) was coated and kept at room temperature for 1h to block the unbound area of the sensor. Finally, the sensor was washed again and stored in the refrigerator until use.

Electrochemical Characterization of the Sensor Stepwise Modification

The electrochemical experiments were performed on a portable commercial potentiostat (Emstat blue, Palmsens), to demonstrate the amenability of the platform for future point-of-care applications. Firstly, cyclic voltammetry was performed to investigate the electrochemical processes at the electrode-solution interface in the presence of 5 mM $[Fe(CN)_6]^{3-/4-}$ in phosphate buffer saline (1X PBS) solution in the potential window of -0.3 to 0.4 V at a scan rate of 50 mVs^{-1}.

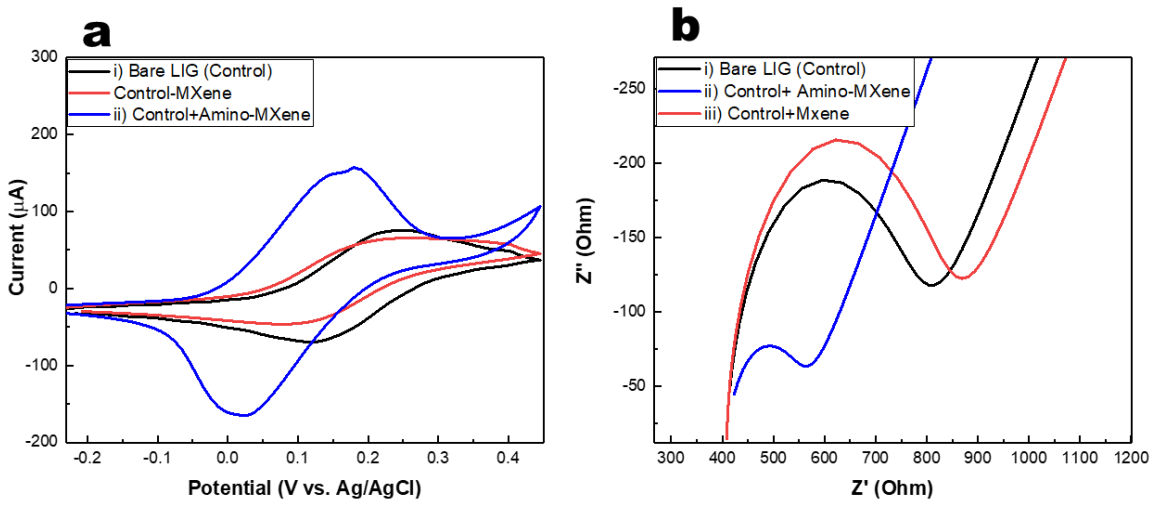

Figure S5. a) CV in the potential window of -0.3 to 0.4 V at 50 mV/s scan rate (5 scans were acquired per condition, with the last scan plotted), and b) Nyquist plot for different stage of sensor modification (3 scans were acquired per condition, with the last scan plotted).

Biosensor Performance with Human Serum Samples

The following experiment was conducted to evaluate the performance of our biosensor using model biological samples, specifically human serum, compared to buffer solutions. Specifically, the buffer samples and human serum samples (diluted to 10% in buffer) were spiked with known concentrations of vit-D, specifically 10 ng mL^{-1}, 50 ng $mL^{-1}$and 100 ng mL^{-1}. The biosensor performance was then analyzed by comparing the analytical signals generated from both sample types. As shown in Figure S5 below, compared to the signals generated from the buffer samples, the serum spike-in samples generated signals with a large (roughly 80%) decrease in signal intensity for all vit-D concentrations. The observed reduction can be attributed to the biofouling of the sensing surface from serum proteins and other biological components. Developing robust antifouling strategies for our platform will be the focus of our future work.

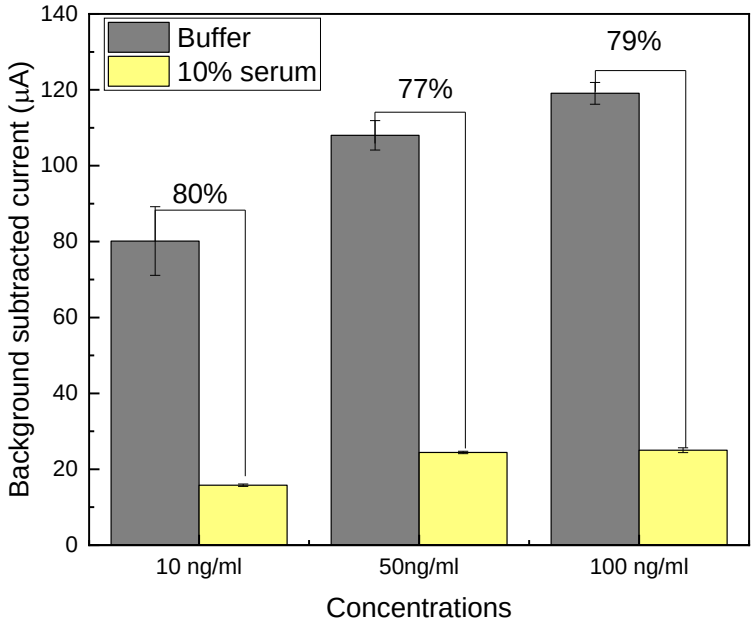

Figure S6. Comparing the biosensor response to three concentrations of vit-D spiked into buffer (grey) versus 10% serum (yellow), with error bars indicating the standard deviation of N=3 data points collected from three DPV scans acquired per concentration.

Table S1. Summary of the peak currents and charge transfer resistance at different stages of surface modification of the vitamin D sensor obtained from Figure 5a and 5b, respectively.

Sample	Peak currents-CV (μA)		Charge transfer resistance_EIS (Ohm)
	anodic	cathodic	
LIG	76	69	405
LIG-Mxene	66	45	463
LIG-Mxene-PEI	102	84	136
LIG-Mxene-PEI-Ab	156	165	152
LIG-Mxene-PEI-Ab-BSA	135	106	302

Table S2. Summary of the literature on electrochemical vit. D biosensors.

Sensor	Method	Dynamic range (ng mL^{-1})	LOD (ng mL^{-1})	Real sample	Ref
BSA/Ab-VD_2/CD-CH/ ITO	DPV	10–50	1.35	-	[3]
Sputtered-Au/SPCE*	i-t	50-200	25	saliva	[4]
BSA/AB-25OHD_3/CAEF/RCP	i-t	10-100	10	serum	[5]
Ab-25OHD/SPE/ FMTAD	SWV	20-200	10	serum	[6]
BSA/Ab-VD_3/Asp-Gd_2O_3NRs/ITO*	DPV	10–100	0.1	serum	[7]
p-PD-Res/SPCE*	SWV	4−801	0.4	plasma	[8]
GCN/β-CD/AuNPs/GCE	DPV	0.1−500	0.01	serum	[9]
Cysg /Au/MoS_2/FTO*	DPV	0.001–0.105	0.038	serum	[10]
MXene-based vit-D Biosensor	DPV	0.1-500	0.001	serum	This work

*Fluoride tin oxide (FTO), Glassy carbon electrode (GCE), Screen printed carbon electrode (SPCE), Indium tin oxide (ITO).

Supplementary References

1. El-Demellawi, J. K., Lopatin, S., Yin, J., Mohammed, O. F. & Alshareef, H. N. Tunable Multipolar Surface Plasmons in 2D Ti 3 C 2 T x MXene Flakes. *ACS*

Nano **12**, 8485–8493 (2018).

2. Barman, S. C. *et al.* Smartphone-Interfaced Electrochemical Biosensor for microRNA Detection Based on Laser-Induced Graphene with π–π Stacked Peptide Nucleic Acid Probes. *ACS Mater. Lett.* **6**, 837–846 (2024).
3. Sarkar, T., Bohidar, H. B. & Solanki, P. R. Carbon dots-modified chitosan based electrochemical biosensing platform for detection of vitamin D. *Int. J. Biol. Macromol.* **109**, 687–697 (2018).
4. Ruiz-Valdepeñas Montiel, V. *et al.* Decentralized vitamin C & D dual biosensor chip: Toward personalized immune system support. *Biosens. Bioelectron.* **194**, 113590 (2021).
5. Chauhan, D. & Solanki, P. R. Hydrophilic and Insoluble Electrospun Cellulose Acetate Fiber-Based Biosensing Platform for 25-Hydroxy Vitamin-D 3 Detection. *ACS Appl. Polym. Mater.* **1**, 1613–1623 (2019).
6. Carlucci, L. *et al.* Several approaches for vitamin D determination by surface plasmon resonance and electrochemical affinity biosensors. *Biosens. Bioelectron.* **40**, 350–355 (2013).
7. Chauhan, D., Kumar, R., Panda, A. K. & Solanki, P. R. An efficient electrochemical biosensor for Vitamin-D3 detection based on aspartic acid functionalized gadolinium oxide nanorods. *J. Mater. Res. Technol.* **8**, 5490–5503 (2019).
8. Kia, S., Bahar, S. & Bohlooli, S. A Novel Electrochemical Sensor Based on Plastic Antibodies for Vitamin D3 Detection in Real Samples. *IEEE Sens. J.* **19**, 4752–4757 (2019).
9. Anusha, T., Bhavani, K. S., Shanmukha Kumar, J. V., Brahman, P. K. & Hassan, R. Y. A. Fabrication of electrochemical immunosensor based on GCN-β-CD/Au nanocomposite for the monitoring of vitamin D deficiency. *Bioelectrochemistry* **143**, 107935 (2022).
10. Kaur, A., Rana, S., Bharti, A., Chaudhary, G. R. & Prabhakar, N. Voltammetric detection of vitamin D employing Au-MoS2 hybrid as immunosensing platform. *Microchim. Acta* **188**, 222 (2021).